Revista Brasileira de Geomática
ISSN: 2317-4285

https://periodicos.utfpr.edu.br/rbgeo

Assessment of Landsat and Sentinel images integration for surface water extent mapping

Heithor Alexandre de Araujo Queiroz
heithor.queiroz@ifbaiano.edu.br
orcid.org/0000-0002-9537-9847
Instituto Federal Baiano (IF Baiano), Guanambi, Bahia, Brasil.

Camylle Vitoria Oliveira Brito
ocamyllevitoria@gmail.com
orcid.org/0000-0001-7900-2823
Instituto Federal Baiano (IF Baiano), Guanambi, Bahia, Brasil.

ABSTRACT

The presence of clouds and shadows and the low temporal resolution of the sensors can be limiting factors for several analyses using satellite images. Considering this, the present study aimed to verify if the integration of the MSI (Sentinel/2) and OLI (Landsat/8) images, aiming at the expansion of the data set, can improve the mapping of the surface water extents of the artificial reservoirs. For this, spectral indices were calculated from images of the OLI and MSI and compared with useful water volume and water depth data collected *in situ* in the Ceraíma reservoir (BA). The correlation *(r)* between the surface water extent values obtained by MSI images and the *in situ* variables useful water volume and relative water depth are 0.80 and 0.78. While, between OLI and the useful water volume and relative water depth variables, the correlations values are 0.59 and 0.58. And, between MSI and OLI, the correlation value is 0.89 and the index of agreement is 0.88. This study concluded that differences in spatial and temporal resolutions have a relevant influence on the ability to integrate images from different satellites for quick and simple results. The low spatial resolution makes it difficult to accurately extract the reservoir contours, while the temporal one limits the number of images for extracting clouds and shadows.

KEYWORDS: Surface water extent. Sentinel 2. MSI. Landsat 8. OLI.

INTRODUCTION

It is estimated that the surface water availability in Brazil varies around 78,600 m³/s, which represents about 30% of the average discharge of all rivers. However, it does not have an equitable distribution in the Brazilian territory, being its largest portion (65,617m³/s) in the Amazon basin, according to the latest update of the country's water resources situation report (AGÊNCIA NACIONAL DE ÁGUAS, 2019). Part of this resource is stored in approximately 19,000 existing artificial reservoirs, and a relevant portion is intended for the production of electricity, as the country's energy matrix is highly dependent on hydroelectricity (JONG et al., 2018; JÚNIOR, 2018). About 50% of the total water withdrawn is applied in irrigation, mainly in the Northeast and Southeast regions, which hold 70% of Brazil's water demand for multiple uses, although they have only 12% of the country's water availability in their territories (POUSA et al., 2019; MORAES et al., 2018; LÉLLIS et al., 2017).

Climatic conditions and geological, topographical, and land use and occupation characteristics, as well as forms of economic and social appropriation of water resources can also be agents of variations in the quantity and quality of water, useful water volume for human consumption and for ecological support, available in continental aquatic systems (lakes, ponds, rivers and reservoirs/dams) (ALTHOFF, RODRIGUES and da SILVA, 2020; ANDRADE et. al., 2019). Therefore, knowing the physical characteristics of aquatic systems, as well as their variations over the years, is of paramount importance for the formulation of public policies (AMORIM and CHAFFE, 2019; MARENGO, TOMASELLA and NOBRE, 2017).

In addition, among the Sustainable Development Goals (SDGs) of the United Nations (UN), there is the item 6.6, which emphasizes the need to prevent the degradation and destruction of aquatic ecosystems, setting as a goal the characterization of variations over time, either on a regional or global scale (UNITED NATIONS, 2018).

However, monitoring these water bodies usually requires high financial investment in the acquisition and maintenance of equipment, such as fluviometric stations and data collection platforms, as well as specialized human resources (AGÊNCIA NACIONAL DE ÁGUAS, 2019; WAGNER, 2000). Therefore, this may make it impossible for the monitoring and evaluation of water resources to be carried out in their entirety, requiring strategies to prioritize the aquatic systems to be observed.

A complementary alternative to conventional water resources monitoring systems is the application of satellite images (eg, CHIPMAN, 2019; MA et al., 2019; OVAKOGLOU et al., 2016), which over the past four decades has allowed the construction of a large dataset on aquatic systems, with unprecedented wealth of spatiotemporal details. This is a result of the growing number of satellite images made available by Earth observation space missions, such as the Landsat and Sentinel missions, and which are mostly free of charge.

In this context, qualitative (LAD, MEHTA and VASHI, 2020; RADU et al., 2020; KUKRER and MUTLU, 2019; RIVA et al., 2019) and quantitative (TULBURE and BROICH, 2019; LI et al., 2018; PRIGENT et al., 2012) studies are recurrent, in which the use of images obtained by multispectral optical sensors, comprising

the visible and infrared bands (400-950 nm) in the electromagnetic spectrum, predominates.

Some studies have stood out in mapping and monitoring the dynamics of surface water extents in continental aquatic systems, predominantly adopting images from a single sensor or a series of very similar sensors belonging to the same space mission. On a global scale, Pickens et al. (2020) used a series of 3.4 million satellite images to assess changes between 1999 and 2018 and Pekel et al. (2016) processed about 3 million images from the 1984-2015 year range. Both adopted images from the Landsat mission alone. On the subcontinental or local scale, Mueller et al. (2016) evaluated 25 years of variation in Australia and Tulbure et al. (2016) analyzed a 30-year interval in the Murray-Darling basin, Australia. Meanwhile, Martins et al. (2019) mapped the dynamics that occurred between 2013 and 2017 in the Sobradinho reservoir, in the semiarid region of Brazil.

Generally, the identification of surface water extents (surface of aquatic systems) is performed from different spectral bands of optical images, based on the principle of distinguishing the reflectance of water, which is low in the infrared channels, with other types of elements of the landscape. Some examples of these methods are density slice (FRAZIER et al., 2000), supervised or unsupervised classifications (OZESMI and BAUER, 2002; MANAVALAN, SATHYANATH and RAJEGOWDA, 1993) and decision trees (OLTHOF, 2017; ACHARYA et al., 2016; SUN, YU and GOLDBERG, 2011). These methods often have classification rules that are complex to interpret and apply, and they are also insufficiently robust to be universally applicable.

On the other hand, a simple and effective way to identify surface water extents is using spectral indices, namely algebraic operations performed with two or more bands, which help in the design and extraction. Among the most used indices are the Normalized Difference Water Index (NDWI, (Green-NIR)/(Green+NIR)) (MCFEETERS, 1996) and the Modified Normalized Difference Water Index (mNDWI, (Green-SWIR1)/(Green) +SWIR1)) (XU, 2006), where Green represents one of the visible spectral bands (530-590 nm), NIR represents the near infrared spectral bands (830-880 nm) and SWIR of the short-wave infrared (above 1500 nm).

The NDWI is considered the first generation of spectral indices for water characterization, being widely used in the first 10 years of the 21st century (CHOWDARY et al., 2008; HUI et al., 2008). Then, it was pointed out in the study by Xu (2006) that the SWIR band may be less sensitive to concentrations of sediments and other optical active constituents in water than the NIR band, which gave rise to the mNDWI, eventually becoming widely used (MOHAMMADI, COSTELLOE and RYU, 2017; CHEN et al., 2014). The mNDWI can enhance open water detection by suppressing and even removing built-up land noise as well as vegetation and soil noise. Plus, there is a growing collection of dozens of algorithms used in the mapping of aquatic systems. According to Pickens et al., 2020, there are 21 algorithms developed and calibrated for images from TM and ETM+ sensors (Landsat 5 and 7) and 36 for images from the Operational Land Imager (OLI) sensor (Landsat 8). Some studies applied part of these algorithms to images obtained from the Sentinel 2 satellite, Multispectral Instrument (MSI) sensor, such as Yang et al. (2017) and Du et al. (2016).

However, there are few studies that adopt a multisensor approach, integrating images from different satellites. Besides, with the large number of free images available, integrating these different sensor products, such as OLI (Landsat 8) and MSI (Sentinel 2), to expand the dataset, becomes a useful option. This alternative, however, can bring particular challenges such as incompatibilities between radiometric (gray levels), spatial (terrain area represented in the pixel), temporal (period of passage of the satellite over the mapped area) and spectral resolutions (quantity and amplitude of the represented electromagnetic spectrum bands).

Therefore, the present study aims to evaluate whether the integration of images from OLI (Landsat 8) and MSI (Sentinel 2) sensors can benefit the quantitative analysis of surface water extents in artificial reservoirs.

MATERIAL

SATELLITE IMAGES

The satellite images were acquired from Earth Engine Data Catalog using its Java Script API. Figure 1 presents the distribution of the 89 images acquired over the months from Dec/2019 to May/2020. The OLI locator (Path and Row) is 218/070 and the MSI (Tile) is T23LQE.

Figure 1 – Distribution of the 89 OLI and MSI images chosen to monthly subset generation from 2019/DEC to 2020/MAY. The green mark "X" in red box indicates MSI and OLI image date match

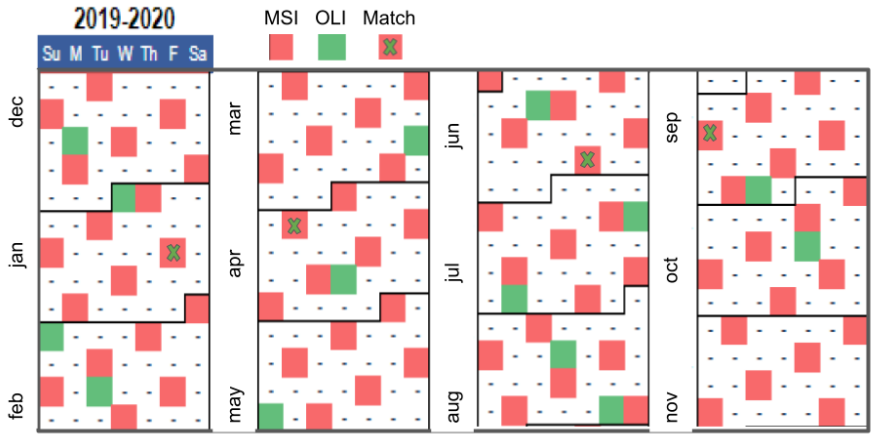

Source: Own authorship (2021).

OLI images from November 2020 were absent in the catalog of Surface Reflectance corrected images. Also, for OLI over December 2019, March, May and October 2020 had only one image.

Landsat 8 (OLI)

Level 2 Surface Reflectance, atmospherically corrected (Bottom of atmosphere – BOA reflectance) to orthorectified data acquired through Earth Engine API (GEE - USGS Landsat 8 Surface Reflectance Tier 1), is chosen to compose the

dataset used to calculate mNDWI spectral index. Level 2 images are post processed results from the georeferenced Landsat Level-1 data that use the Global Land Survey (GLS) database as the primary source for the Ground Control Point (GCP). Here are downloaded 71 images from sensor OLI over 2019 December and 2020 over the months January and November in Green and Short-Wave Infrared (SWIR1) bands with spatial and temporal resolution of 30 m and 16 days respectively. The images were collected without cloud cover limit. Then, monthly subset were obtained from cloud mask preprocessing. Here, this set of images is used to detect water surface changes occurrence over the study area.

Sentinel 2 (MSI)

Level-2A Bottom-Of-Atmosphere (BOA), atmospherically corrected orthoimage reflectance product, from Copernicus Sentinel-2 satellites (S2A and S2B) is chosen to compose the dataset used to calculate the mNDWI spectral index, since it provides relatively high spatialtemporal resolution (10/20/60 m-5 days), with 13 multispectral bands through its on board MSI sensor. Here are downloaded 18 images over 2019 December and 2020 over the months January and November, in two bands: 10 m resolution band Green and 20 m SWIR1. The images were collected without cloud cover limit. Then, monthly subset were obtained from cloud mask preprocessing. Here, this set of images is also used to detect water surface changes.

IN SITU DATA FROM THE NATIONAL WATER AGENCY (ANA)

Useful water volume (%) and water depth (m) data were acquired from the Reservoir Monitoring System (SAR) of the National Water Agency (ANA – Agência Nacional de Águas in portuguese), which operates and maintains the Northeast and Semi-Arid module (https://www.ana.gov.br/sar/), launched at the end of 2019, in which more than 500 reservoirs are monitored in the nine states of the Northeast Region and in Minas Gerais, with a total capacity close to 40 billion m³.

Figure 2 – In situ data acquisition website interface

Source: Own authorship (2021).

STUDY AREA

The chosen study area was the Ceraíma reservoir (Figure 3), which arose from the dam in the course of the Carnaíba de Dentro River, in the São Francisco

River Basin, located in the limits of the municipality of Guanambi/BA, at latitude 14° 17' 2.86" S and longitude 42° 40' 52.38" W. The Dam is operated by the public company Companhia de Desenvolvimento dos Vales do São Francisco and Parnaíba (CODEVASF). The types of demands met include urban human supply (33%), rural human supply (15%), animal watering (14%) and irrigation (38%). It supplies the Bahia cities of Candiba, Guanambi, Igaporã and Pindaí, in addition to the irrigated perimeter of Ceraíma. Being, therefore, of great relevance for the water and food security of the region.

Figure 3 – Study area: (a) Ceraíma dam location in Bahia State, Brazil (b) MSI true color composition (RGB 4; 3; 2); (c) monthly mean precipitation in São Francisco River catchment area from 2019/DEC to 2020/NOV. Precipitation is acquired from Climate Hazards Group InfraRed Precipitation with Station data (CHIRPS)

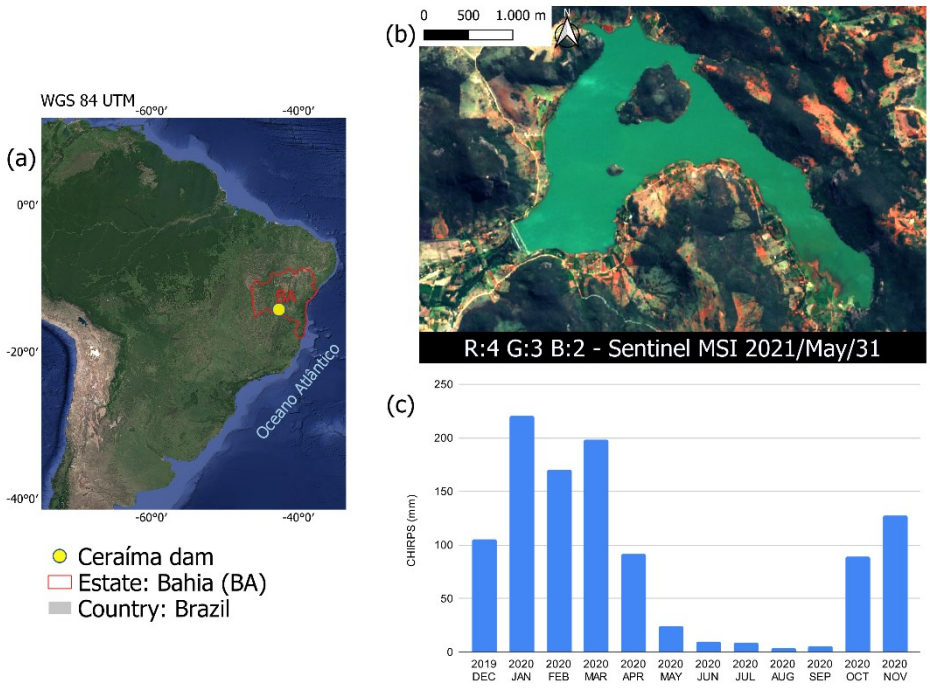

Source: Own authorship (2021).

METHODS

A summary of the dataset and methods is presented in Figure 4. The whole process has been developed in Java Script API environment and QGIS software.

Figure 4 – Methodological steps fluxogram

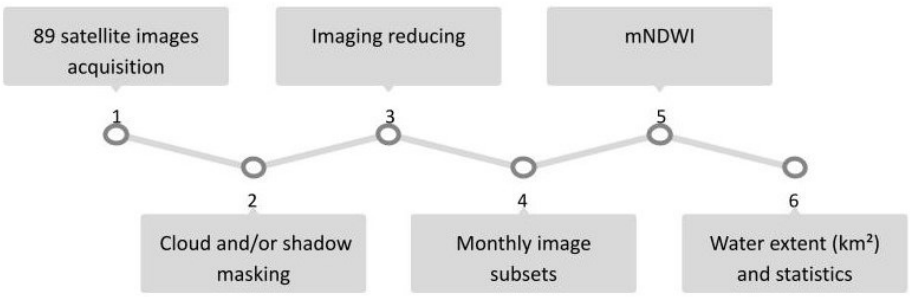

Source: Own authorship (2021).

CLOUD AND SHADOW MASKS

Functions were applied to mask clouds based on the bands pixel_qa of OLI Landsat 8 and QA60 of MSI Sentinel. It helps to flag cloud shadow and cloud pixels from OLI and clouds and cirrus pixel from MSI images that are disregarded in image subset generation.

MONTHLY IMAGE SUBSETS

To aggregate masked images in only one monthly subset it is required to reduce the collection, which means the adoption of a statistical function to choose each pixel of the final image subset. Here the widely used statistics Median is adopted, i.e., "the middle" value that separates the higher half from the lower half of a data sample and disregard the masked pixels.

WATER EXTENT MAPPING STATISTICS

The water extent mapping was performed with a simple threshold on the spectral index images: mNDWI>0, where NDWI=(GREEN – SWIR1)/(GREEN+SWIR1). The proposed approach enables an effective and fast mapping of water extent in the Ceraima reservoir. These indexes are widely used in remote sensing applications, which makes it easy to replicate in other studies in which no machine learning technics are required. Then, from the water extent mNDWI-derived of OLI and MSI, it was calculated the area in square kilometer (km²) for each month assessed. Also, Shapiro-Wilk test, t-student, Pearson correlation coefficient *(r)* and the index of agreement was computed to assess the normal distribution, and the degrees of relationship between the variables assessed.

RESULTS

Figure 5 shows the surface water extent of the Ceraíma reservoir, extracted from the mNDWI, in the months where the lowest and highest records of usable volume and relative water depth occurred, identified by ANA's *in situ* surveys. It is visually noticeable a similarity in the identification of the water surface boundaries using distinct images of the OLI (Figure 5 a, and b) and MSI (Figure 5 c, and d) sensors.

Considering a 6-month interval (Dec/2019 to May/2020), the southeast part of the Ceraíma reservoir presents a marked variation in terms of the presence or absence of a water surface since it remains flooded in periods of higher volume and relative water depth. This is mainly motivated by the shallow depth of this stretch of the reservoir. This occurrence is highlighted in Figures 6 and 7, which show the difference in performance, in the delineation of the edges of the reservoir, between the mNDWI extracted from the images of OLI and MSI sensors.

Figure 5 – Surface water extent mNDWI-derived of Ceraíma dam when the smaller (2019/DEC) and larger (2020/MAY) in situ data were recorded from useful water volume and water depth

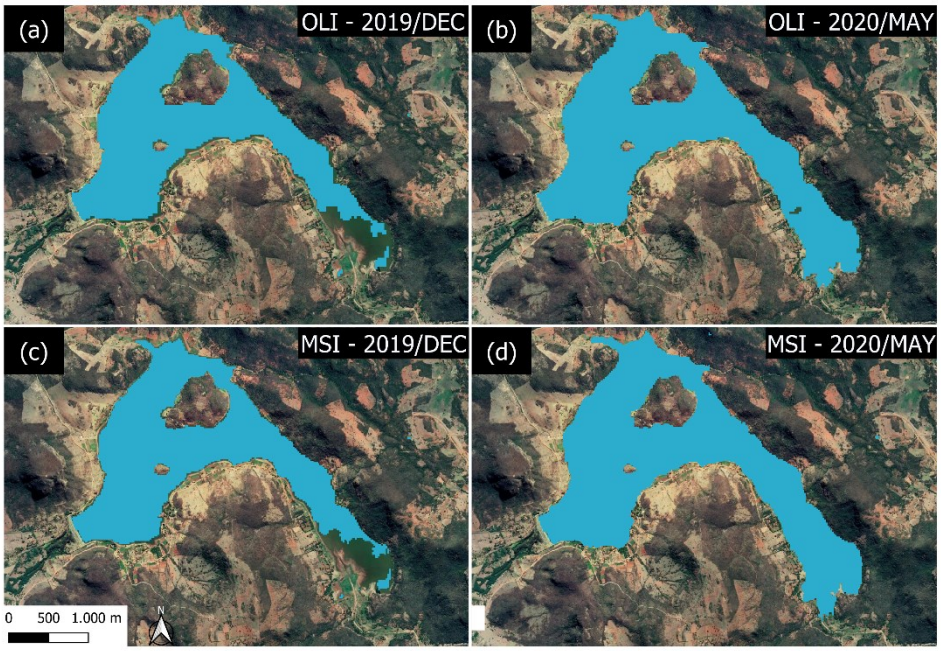

Source: Own authorship (2021).

Figure 6 – OLI and MSI performance differences in Ceraíma dam edge extraction mNDWI-derived over 2019/DEC, highlithed in the frames a, b, c, d, e and f

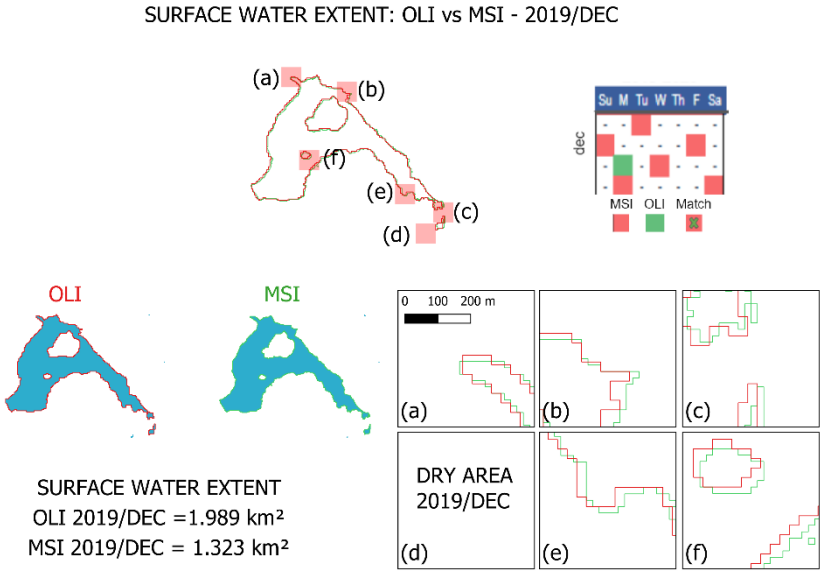

Source: Own authorship (2021).

The 30 meter-spatial resolution of the OLI images makes the contours less smooth. Also, the area values calculated from each image are distinct. Six MSI images and one OLI image were used here, without match dates (Figures 6 and 7). Figure 6 shows that while the surface water extent value calculated from MSI images for the month of Dec/2019 is 1.323km², from OLI images it is 1.989 km²

for the same period. In Figure 7, on the other hand, is presented for the period May/2020, when compared to Dec/2019, a smaller difference between the values obtained from OLI and MSI images, but still relevant, being the area value of the surface water extent of 3.488 km² (OLI) and 3.626 km² (MSI).

Figure 7 – OLI and MSI performance differences in Ceraíma dam edge extraction mNDWI-derived over MAY/2020, highlithed in the frames a, b, c, d, e and f

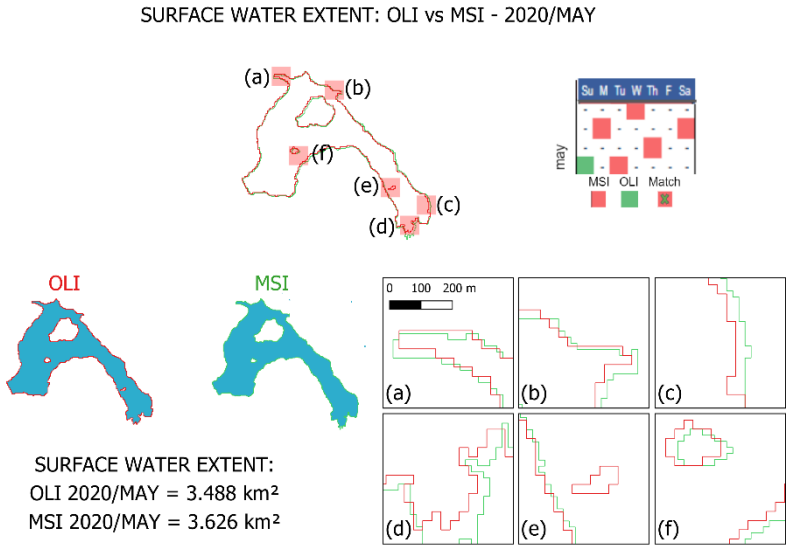

Source: Own authorship (2021).

In Figure 8 are shown the monthly values, in the period between Dec/2019 and Nov/2020, of the area of the surface water extent extracted from the MSI and OLI images and the data collected *in situ* by ANA, representing monthly useful water volume (%) and relative water depth (%). The relative water depth values, usually shown in meters, were here normalized to the variations that occurred in the period for better visual presentation in the chart. Thus, considering variations between 511 and 515 meters of elevation, they correspond in Figure 8 to the minimum values, 0%, and maximum values, 100%, respectively.

Figure 8 – Monthly comparison over DEC/2019 to NOV/2020 of surface water extent mNDWI-derived (MSI and OLI) and in situ dataset of monthly useful water volume and water depth

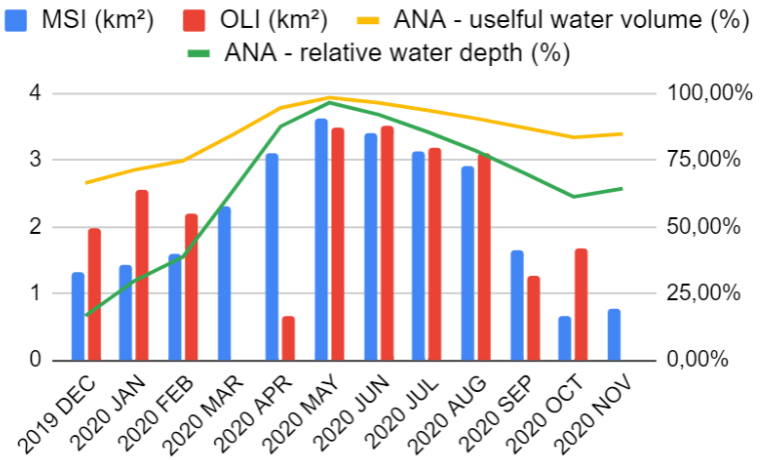

Source: Own authorship (2021).

There was difficult to achieve the dataset (images and *in situ)* in an ideal scenario of match dates. Then, it was opted to obtain monthly reduced subsets aiming to minimize the gaps of data. Still, front of the high percentage of cloud, the images of March, April and November were not considered for statistical analysis.

Shapiro-Wilk test shows the p-value for OLI of 0.929 and for MSI of 0.897, retaining the hypothesis that the data is normally distributed. Also, p-value of 0.03 from t-student, shows significant relationship between OLI and MSI with 95% of confidence level. In Table 1 are shown the calculated Pearson's correlation coefficient *(r)* values and evidences the direct correlation between the intra-annual variations detected by the mNDWI of the MSI images, with *r* equal to 0.80 of the useful water volume and 0.78 of the relative water depth of the reservoir.

Tabela 1 – Pearson' correlation *(r)* of surface water extent mNDWI-derived (MSI and OLI) and *in situ* dataset of useful water volume and relative water depth

	OLI mNDWI	MSI mNDWI	ANA volume útil	ANA cota
OLI mNDWI	1			
MSI mNDWI	0.89	1		
ANA uselful volume	0.59	0.80	1	
ANA relative depth	0.58	0.78	1	1

Source: Own authorship (2021).

In comparison, *r* values between the mNDWI of the OLI images and the *in situ* data are directly correlated with lower values. Also *r* value and the index of agreement between MSI and OLI km² surface water extents is 0.89 and 0.88, respectively.

DISCUSSION

The rainfall regime of the southwest region of Bahia in the evaluated seasonal cycle from Dec/2019 to Nov/2020, the region where the Ceraíma reservoir is located, presented a higher rainfall in the summer, from December to March, until the middle of the fall period. Consequently, the discharges from the reservoirs in the post-rain period are controlled to store water and ensure water security for the population and the like. This was directly reflected in the useful water and relative water depth values recorded by ANA equipment installed *in situ*, as seen in Figures 5, 6, 7 and 8.

In Figures 6 and 7, in which visual comparisons allow detecting differences between the delineation of the edges of the Ceraíma reservoir, in the periods of minimum and maximum water availability records, it can be inferred that in addition to the influence of visually evident differences in resolution 10 m (MSI) and 30 m (OLI) spatial resolution, the temporal resolution, which comprises the satellite revisit interval, can add some square meters of error in quantification, considering the advance or retreat of the edge line directly proportional to the useful water and the relative water depth.

Considering the lack of systematized data for the Ceraíma region that represents the surface area of the reservoir's surface water extents, which could serve as validation data for the evaluations in this study, the variables useful water volume and relative water depth were adopted. The first represents the amount of water in the reservoir that can be pumped, which is a volumetric variable. The second, relative water depth, estimates a relation of the distance between the reservoir bottom and the surface water extent, thus being a linear variable. Therefore, inaccuracies in the analyses can be added considering the structural differences of the adopted parameters. On the other hand, the values presented in Table 1 and Figure 8 may corroborate the visual differences shown in Figures 5, 6 and 7.

Among the 89 images used in this annual analysis, 18 were from OLI. Considering the common variability that occur in artificial reservoirs, the low date match rate (3 dates) between MSI and OLI images aggregates limitations to perform the analysis. On the other hand, it is a rich opportunity for the data offering, once the other 15 OLI images may fill data gaps in other 15 days that MSI do not provide, being used to produce information on the water surface.

CONCLUSIONS

This study aimed to evaluate whether a simple and fast integration of images from the OLI and MSI sensors, onboard the Landsat 8 and Sentinel 2 satellites, could be an alternative to quantify the area of surface water extents from surface water systems. The approach adopted has the benefit of expanding the dataset, mitigating the effects of the presence of clouds and shadows and the low temporal resolution of the sensors, being tested in the artificial reservoir of Ceraíma/BA.

The number of Sentinel images was crucial to minimize the image gaps, and make it possible to mask clouds in all the months assessed. It was concluded that the differences in spatial and temporal resolutions have a relevant influence on the ability to integrate images from different satellites to obtain results. The low spatial resolution makes it difficult to automatically extract the contours of the reservoirs accurately, while the temporal one limits the number of images considerably for extracting clouds and shadows.

In spite of the simple integration between the OLI and MSI images for the mapping of surface water extents, thus, making the visualization of intra-annual dynamics possible, it is recommended evaluating the possibility of fusion bands of the Landsat Green and SWIR1 with the panchromatic of 15 meters, mainly for applications that aim to use the surface water extents area in order to support the estimate of surface water availability. The goal is to optimize the spatial resolution and minimize the effects of differences in resolution on area values of surface water extents.

For further research, it is suggested to evaluate the influence of differences between radiometric and spectral resolutions of images from different sensors. This investigation can produce an optimization in the integration of images from these important OLI and MSI sensors and leverage advances in current aquatic studies.

Avaliação da integração de imagens Landsat e Sentinel no mapeamento de espelho d'água

RESUMO

A presença de nuvens e sombras e a baixa resolução temporal dos sensores podem ser fatores limitantes para as análises usando imagens de satélites. Considerando isso, o presente estudo almejou verificar se a integração das imagens dos sensores MSI (Sentinel 2) e OLI (Landsat 8), visando a ampliação do conjunto de dados, pode aprimorar o mapeamento dos espelhos d'água dos reservatórios artificiais. Para isso, foram calculados índices espectrais a partir de imagens OLI e MSI e comparados com dados de volume útil e cota coletados *in situ* no reservatório de Ceraíma (BA). A correlação *(r)* entre os valores de espelho d'água obtidos por imagens MSI e as variáveis *in situ* volume útil e cota são de 0,80 e 0,78. Enquanto, entre OLI e as variáveis volume útil e cota, os valores de correlação são 0,59 e 0,58. E entre MSI e OLI, *r* é de 0,89 e o índice de concordância é de 0,88. Este estudo concluiu que as diferenças de resoluções espaciais e temporais têm uma relevante influência na capacidade de integração entre as imagens de diferentes satélites para obtenção rápida e simples de resultados. A baixa resolução espacial dificulta a extração precisa dos contornos do reservatório, enquanto a temporal limita a quantidade de imagens de forma considerável para extração de nuvens e sombras.

PALAVRAS-CHAVE: Espelhos d'água. Sentinel 2. MSI. Landsat 8. OLI.

ACKNOWLEDGEMENT

Thanks to the National Council for Scientific and Technological Development (CNPq) and the Pro-Rectory of Research and Innovation (PROPES) of the Federal Institute of Education, Science and Technology of Bahia (IF Baiano), which through Notice No. 69/2020, Internal Call PROPES Nº 10/2020 granted financial support to the research project of the Study Group in Applied Geotechnologies (GREGA) led by the 1st author and scientific initiation scholarship (PIBIC) to the co-author of this article.

BIBLIOGRAPHY

ACHARYA, T. D.; LEE, D. H.; YANG, I. T.; LEE, J. K. Identification of water bodies in a Landsat 8 OLI image using a J48 decision tree. **Sensors**, v. 16, n. 7, p. 1075, 2016. https://doi.org/10.3390/s16071075.

AGÊNCIA NACIONAL DE ÁGUAS (BRASIL). Conjuntura dos recursos hídricos no Brasil 2019: informe anual /Agência Nacional de Águas. Brasília: ANA, 2019.

ALTHOFF, D.; RODRIGUES, L. N.; DA SILVA, D. D. Impacts of climate change on the evaporation and availability of water in small reservoirs in the Brazilian savannah. **Climatic Change**, v. 159, n. 2, p. 215-232, 2020. https://doi.org/10.1007/s10584-020-02656-y.

AMORIM, P. B.; CHAFFE, P. B. Towards a comprehensive characterization of evidence in synthesis assessments: the climate change impacts on the Brazilian water resources. **Climatic Change**, v. 155, n. 1, p. 37-57, 2019. https://doi.org/10.1007/s10584-019-02430-9.

ANDRADE, E. P. et al. Water scarcity in Brazil: part 1—regionalization of the AWARE model characterization factors. **The International Journal of Life Cycle Assessment**, p. 1-17, 2019. https://doi.org/10.1007/s11367-019-01643-5.

CHEN, Y. et al. Estimate of flood inundation and retention on wetlands using remote sensing and GIS. **Ecohydrology**, v. 7, n. 5, p. 1412-1420, 2014. https://doi.org/10.1002/eco.1467.

CHIPMAN, J. W. A multisensor approach to satellite monitoring of trends in lake area, water level, and volume. **Remote Sensing**, v. 11, n. 2, p. 158, 2019. https://doi.org/10.3390/rs11020158.

CHOWDARY, V. M. et al. Assessment of surface and sub-surface waterlogged areas in irrigation command areas of Bihar state using remote sensing and GIS. **Agri-**

cultural water management, v. 95, n. 7, p. 754-766, 2008. https://doi.org/10.1016/j.agwat.2008.02.009.

DU, Y. et al. Water bodies' mapping from Sentinel-2 imagery with modified normalized difference water index at 10-m spatial resolution produced by sharpening the SWIR band. **Remote Sensing**, v. 8, n. 4, p. 354, 2016. https://doi.org/10.3390/rs8040354.

FRAZIER, P. S. et al. Water body detection and delineation with Landsat TM data. **Photogrammetric engineering and remote sensing**, v. 66, n. 12, p. 1461-1468, 2000.

HUANG, C. et al. Detecting, extracting, and monitoring surface water from space using optical sensors: A review. **Reviews of Geophysics**, v. 56, n. 2, p. 333-360, 2018. https://doi.org/10.1029/2018RG000598.

HUI, F. et al. Modelling spatial-temporal change of Poyang Lake using multitemporal Landsat imagery. **International Journal of Remote Sensing**, v. 29, n. 20, p. 5767-5784, 2008. https://doi.org/10.1080/01431160802060912.

JONG, P. et al. Hydroelectric production from Brazil's São Francisco River could cease due to climate change and inter-annual variability. **Science of the Total Environment**, v. 634, p. 1540-1553, 2018. https://doi.org/10.1016/j.scitotenv.2018.03.256.

JÚNIOR, W. C. de S. Water and Energy Nexus under Climate Change Scenarios: Lessons from Brazil. **New Water Policy & Practice**, v. 4, n. 2, p. 7-18, 2018. https://doi.org/10.18278/nwpp.4.2.2.

KÜKRER, S.; MUTLU, E.. Assessment of surface water quality using water quality index and multivariate statistical analyses in Saraydüzü Dam Lake, Turkey. **Environmental monitoring and assessment**, v. 191, n. 2, p. 71, 2019. https://doi.org/10.1007/s10661-019-7197-6.

LAD, D.; MEHTA, M.; VASHI, M. **Assessment of Surface Water Quality Using GIS: Case of Tapi Basin, Surat, Gujarat, India**. In: Applications of Geomatics in Civil Engineering. Springer, Singapore, 2020. p. 303-311. https://doi.org/10.1007/978-981-13-7067-0_24.

LÉLLIS, B. C. et al. Effective management of irrigation water for carrot under constant and optimized regulated deficit irrigation in Brazil. **Agricultural Water Management**, v. 192, p. 294-305, 2017. https://doi.org/10.1016/j.agwat.2017.07.018.

LI, L. et al. Monitoring the dynamics of surface water fraction from MODIS time series in a Mediterranean environment. **International journal of applied earth observation and geoinformation**, v. 66, p. 135-145, 2018. https://doi.org/10.1016/j.jag.2017.11.007.

MA, Y. et al. Estimating water levels and volumes of lakes dated back to the 1980s using Landsat imagery and photon-counting lidar datasets. **Remote Sensing of Environment**, v. 232, p. 111287, 2019. https://doi.org/10.1016/j.rse.2019.111287.

MANAVALAN, P.; SATHYANATH, P.; RAJEGOWDA, G. L. Digital image analysis techniques to estimate waterspread for capacity evaluations of reservoirs. **Photogrammetric Engineering and Remote Sensing**, v. 59, n. 9, p. 1389-1395, 1993.

MARENGO, J. A.; TOMASELLA, J.; NOBRE, C. A. **Climate change and water resources**. In: Waters of Brazil. Springer, Cham, 2017. p. 171-186. https://doi.org/10.1007/978-3-319-41372-3_12.

MARTINS, V. S. et al. Remote sensing of large reservoir in the drought years: Implications on surface water change and turbidity variability of Sobradinho reservoir (Northeast Brazil). **Remote Sensing Applications: Society and Environment**, v. 13, p. 275-288, 2019. https://doi.org/10.1016/j.rsase.2018.11.006.

MCFEETERS, S. K. The use of the Normalized Difference Water Index (NDWI) in the delineation of open water features. **International journal of remote sensing**, v. 17, n. 7, p. 1425-1432, 1996. https://doi.org/10.1080/01431169608948714.

MOHAMMADI, A.; COSTELLOE, J. F.; RYU, D. Application of time series of remotely sensed normalized difference water, vegetation and moisture indices in characterizing flood dynamics of large-scale arid zone floodplains. **Remote sensing of Environment**, v. 190, p. 70-82, 2017. https://doi.org/10.1016/j.rse.2016.12.003.

MORAES, M. M. G. A. et al. The impact of global change on economic values of water for Public Irrigation Schemes at the São Francisco River Basin in Brazil. **Regional Environmental Change**, v. 18, n. 7, p. 1943-1955, 2018. https://doi.org/10.1007/s10113-018-1291-0.

MUELLER, N. et al. Water observations from space: Mapping surface water from 25 years of Landsat imagery across Australia. **Remote Sensing of Environment**, v. 174, p. 341-352, 2016. https://doi.org/10.1016/j.rse.2015.11.003.

OLTHOF, I. Mapping seasonal inundation frequency (1985–2016) along the St-John River, New Brunswick, Canada using the Landsat archive. **Remote Sensing**, v. 9, n. 2, p. 143, 2017. https://doi.org/10.3390/rs9020143.

OVAKOGLOU, G. et al. Use of MODIS satellite images for detailed lake morphometry: Application to basins with large water level fluctuations. **International journal of applied earth observation and geoinformation**, v. 51, p. 37-46, 2016. https://doi.org/10.1016/j.jag.2016.04.007.

OZESMI, S. L.; BAUER, M. E. Satellite remote sensing of wetlands. **Wetlands ecology and management**, v. 10, n. 5, p. 381-402, 2002. https://doi.org/10.1023/A:1020908432489.

PEKEL, J. et al. High-resolution mapping of global surface water and its long-term changes. **Nature**, v. 540, n. 7633, p. 418-422, 2016. https://doi.org/10.1038/nature20584.

PICKENS, A. H. et al. Mapping and sampling to characterize global inland water dynamics from 1999 to 2018 with full Landsat time-series. **Remote Sensing of Environment**, v. 243, p. 111792, 2020. https://doi.org/10.1016/j.rse.2020.111792.

POUSA, R. et al. Climate Change and Intense Irrigation Growth in Western Bahia, Brazil: The Urgent Need for Hydroclimatic Monitoring. **Water**, v. 11, n. 5, p. 933, 2019. https://doi.org/10.3390/w11050933.

PRIGENT, C. et al. Changes in land surface water dynamics since the 1990s and relation to population pressure. **Geophysical Research Letters**, v. 39, n. 8, 2012. https://doi.org/10.1029/2012GL051276.

RADU, V. et al. Overall assessment of surface water quality in the Lower Danube River. **Environmental Monitoring and Assessment**, v. 192, n. 2, p. 135, 2020. https://doi.org/10.1007/s10661-020-8086-8.

RIVA, F. et al. Risk assessment of a mixture of emerging contaminants in surface water in a highly urbanized area in Italy. **Journal of hazardous materials**, v. 361, p. 103-110, 2019. https://doi.org/10.1016/j.jhazmat.2018.07.099.

SUN, D.; YU, Y.; GOLDBERG, M. D. Deriving water fraction and flood maps from MODIS images using a decision tree approach. **IEEE Journal of Selected Topics in Applied Earth Observations and Remote Sensing**, v. 4, n. 4, p. 814-825, 2011. https://doi.org/10.1109/JSTARS.2011.2125778.

TULBURE, M. G. et al. Surface water extent dynamics from three decades of seasonally continuous Landsat time series at subcontinental scale in a semi-arid region. **Remote Sensing of Environment**, v. 178, p. 142-157, 2016. https://doi.org/10.1016/j.rse.2016.02.034.

TULBURE, M. G.; BROICH, Mark. Spatiotemporal patterns and effects of climate and land use on surface water extent dynamics in a dryland region with three decades of Landsat satellite data. **Science of The Total Environment**, v. 658, p. 1574-1585, 2019. https://doi.org/10.1016/j.scitotenv.2018.11.390.

UNITED NATIONS (UN). Sustainable Development Goal 6 Synthesis Report on Water and Sanitation. United Nations, New York, 2018. Available in <https://www.unglobalcompact.org/library/5623>. acessed in 02 August 2021.

XU, H. Modification of normalized difference water index (NDWI) to enhance open water features in remotely sensed imagery. **International Journal of Remote Sensing**, v. 27, n. 14, p. 3025-3033, 2006. https://doi.org/10.1080/01431160600589179.

WAGNER, R. J. Guidelines and standard procedures for continuous water-quality monitors: Site selection, field operation, calibration, record computation, and reporting. US Department of the Interior, US Geological Survey, 2000. https://doi.org/10.3133/tm1D3.

YANG, X. et al. Mapping of urban surface water bodies from Sentinel-2 MSI imagery at 10 m resolution via NDWI-based image sharpening. **Remote Sensing**, v. 9, n. 6, p. 596, 2017. https://doi.org/10.3390/rs9060596.

Recebido: 02 ago. 2021
Aprovado: 04 nov. 2021
DOI: 10.3895/rbgeo.v10n1.14590
Como citar: QUEIROZ, H. A. A.; BRITO, C. V. O. Assessment of Landsat and Sentinel integration for surface water extent mapping. **R. bras. Geom.**, Curitiba, v. 10, n. 1, p. 003-019, jan./mar. 2022. Disponível em: <https://periodicos.utfpr.edu.br/rbgeo>. Acesso em: XXX.
Correspondência:
Heithor Alexandre de Araújo Queiroz
Rua K, 144, CEP 46430-000, Guanambi, Bahia, Brasil.